Inorganic Chemistry

Article

pubs.acs.org/IC

Hydration Properties and Ionic Radii of Actinide(III) Ions in Aqueous Solution

Paola D'Angelo,*[,†] Fausto Martelli,[‡,§] Riccardo Spezia,[§] Adriano Filipponi,[∥] and Melissa A. Denecke[⊥]

[†]Department of Chemistry, University of Rome "La Sapienza", P. le A. Moro 5, 00185 Roma, Italy

[‡]Frick Chemistry Laboratory, Department of Chemistry, Princeton University, Princeton New Jersey 08540, United States

[§]Laboratoire Analyse et Modélisation pour la Biologie et l'Environnement, UMR 8587 CNRS-CEA-UEVE, Université d'Evry Val d'Essonne, Bd F. Mitterrand, 91025 Evry Cedex, France

[∥]Dipartimento di Scienze Fisiche e Chimiche, Università degli Studi dell'Aquila, Via Vetoio, 67100 L'Aquila, Italy

[⊥]Institut für Nukleare Entsorgung, Forschungszentrum Karlsruhe, P.O. Box 3640, 76021, Karlsruhe, Germany

Supporting Information

ABSTRACT: Ionic radii of actinide(III) cations (from U(III) to Cf(III)) in aqueous solution have been derived for the first time starting from accurate experimental determination of the ion−water distances obtained by combining extended X-ray absorption fine structure (EXAFS) results and molecular dynamics (MD) structural data. A strong analogy has been found between the lanthanide and actinide series concerning hydration properties. The existence of a contraction of the An−O distance along the series has been highlighted, while no decrease of the hydration number is evident up to Cf(III).

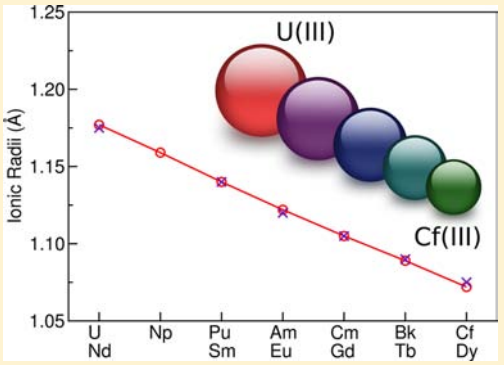

1. INTRODUCTION

An in-depth understanding of the solution chemistry of actinide ions is extremely important for nuclear technology and nuclear waste disposal. The aqueous chemistry of An(III) (An = actinide) systems is of special importance since +3 is the thermodynamically most stable oxidation state for heavy actinides. Detailed information on the An(III) hydration properties, also in comparison with those of the Ln(III) (Ln = lanthanide) aqua ions, is essential for separation chemistry and prediction of the potential for actinide migration from a nuclear waste repository into natural aquifers. Full characterization of electrolyte solutions in terms of their thermodynamic, structural, transport, and spectroscopic properties requires knowledge of the ability of the solvent to approach a given ion, which is strictly dependent on its ionic radius. In many cases, the "crystal ionic radii" reported by Shannon[1] are employed to derive ion properties in electrolyte solutions, even if it is not clear if the radii of ions determined in crystalline compounds are transferable to ions in solution. In particular, packing effects in crystals are expected to have an influence on the bond distance distribution; for this reason, ionic radii in solution have been derived by some authors starting from experimental distances obtained from solution studies.[2,3] While the determination of bond distances is quite straightforward for crystalline samples, the characterization of structures in liquid systems is more challenging and difficult to obtain using standard experimental techniques. Extended X-ray absorption fine structure (EXAFS) spectroscopy is the structural probe of choice for characterization of ion coordination in dilute solutions because of its intrinsic chemical specificity and short-range sensitivity. However, proper extraction of the structural parameters from the EXAFS experimental signal rests on the use of reliable starting models that can be obtained, for example, from molecular dynamics (MD) simulations.[4−9] Recently, a polarizable classical interaction potential has been specifically developed by some of us to study An(III) ions in liquid water.[10] From this MD investigation, the hydration properties of the actinide series have been determined. In addition, a revised set of ionic radii in aqueous solution has been derived for Ln(III) cations, and, owing to the lanthanide contraction, a regular decrease of the ionic radii has been observed along the series.[11,12] A similar trend is expected also for the actinide series, but up to now experimental determination of the actinide ionic radii in aqueous solution is still lacking.[13] This is mainly due to the great experimental difficulty in studying actinide aqueous solutions, owing to the redox instability of the lighter An(III) aqua ions. As a consequence, a systematic experimental investigation of the hydration properties of the whole actinide series is not available in the literature, and a clear and unique picture is still missing. The hydration structure of the U(III), Np(III), and Pu(III)

Received: March 19, 2013
Published: August 27, 2013

ions was recently determined based on EXAFS data,[14−17] while the coordination geometry of the heavier An(III) aqua ions from Am(III) to Cf(III) has been derived by different research groups, showing a decrease in the An−O distance across the series.[18−24] The coordination number values determined experimentally are not homogeneous, ranging from 8 to 10.[13,18−24] From the theoretical point of view, the previously mentioned MD simulations[10] report a coordination number of 9 for light actinide ions and 8 for heavy ones, in agreement with other studies on Cm(III) by Gagliardi and co-workers[25] and de Jong and co-workers,[26] who reported a coordination number 9 as the most likely. Quantum chemical calculations on clusters with implicit solvation reported by Dolg and co-workers[27] examined different coordination motifs, but they were not conclusive on this point. Herein, we report a complete and unified analysis of the hydration properties of the actinide series from U(III) to Cf(III). We also present the first determination of ionic radii of An(III) ions in aqueous solution obtained by coupling newly refined EXAFS data and state of the art MD simulations.

2. EXPERIMENTAL SECTION

2.1. Molecular Dynamics Simulations. MD simulations were carried out by modeling the total potential energy as a sum of different terms:

$$V_{tot} = V_{elec} + V^{LJ}_{O-O} + V_{An-O} \quad (1)$$

where V_{elec} is the electrostatic energy term composed of Coulomb and a polarization term following the Thole's induced dipole model.[28] V^{LJ}_{O-O} is the 12−6 Lennard−Jones potential describing the O−O interaction. Because of the explicit polarization introduced in the model, the original TIP3P[29] was modified into the TIP3P/P water model;[30] that is, the charges on O and H were rescaled to reproduce correctly the dipole moment of liquid water. Atomic polarizability directly enters into the polarization part of the electrostatic energy term, and we use values obtained from ab initio calculations as detailed in ref 10. V_{An-O} accounts for the nonelectrostatic An−O interaction potential. We have used a potential composed by a long-range attractive part with a $1/r^6$ behavior and a short-range repulsive part modeled via an exponential function, dealing with the well-known Buckingham potential:

$$V_{An-O} = A_{An-O}\exp(-B_{An-O}r_{An-O}) - \frac{C_{An-O}}{r^6_{An-O}} \quad (2)$$

Detailed description of parameters developed was reported recently in ref 10, and they are listed in Table S1 of Supporting Information.

Each MD simulation consists of one An(III) ion and 216 rigid water molecules in a cubic box (with edges of 18.64 Å) at room temperature. As previously reported, MD simulations with a 1000 water molecule box provide the same cation structural and dynamical hydration properties as the simulation with 216 water molecules.[31−33] Therefore, simulations with 216 water molecules were used to assess hydration properties of the whole An(III) series.

Periodic boundary conditions were applied to the simulation box in order to mimic the hydration of an ion in liquid water. Long-range interactions were calculated by using the smooth particle mesh Ewald method.[34] The extended Lagrangian method was used to propagate induced dipoles in time.[35] Equations of motion were numerically integrated using a 1 fs time step by means of a velocity-Verlet-based multiple time step algorithm. Initial configurations were built from an equilibrated box with 216 water molecules in which the ion was placed at the center of the box. The system was equilibrated at 298 K for 2 ps. Production runs were subsequently collected for 3 ns. Simulations of hydrated An(III) ions were carried out in the microcanonical NVE ensemble with the classical molecular dynamics (CLMD) code MDVRY.[36] All other simulation details are the same as reported previously.[10,31,37,38]

The structural properties of the actinide aqueous solutions obtained from the simulations are described in terms of radial distribution functions, $g_{An-O}(r)$ and $g_{An-H}(r)$:

$$g_{AB}(r) = \frac{\langle\rho_B(r)\rangle}{\langle\rho_B\rangle_{local}} = \frac{1}{N_A\langle\rho_B\rangle_{local}}\sum_{i=1}^{N_A}\sum_{j=1}^{N_B}\frac{\delta(r_{ij}-r)}{4\pi r^2} \quad (3)$$

where $\langle\rho_B(r)\rangle$ is the particle density of type B at distance r around type A, and $\langle\rho_B\rangle_{local}$ is the particle density of type B averaged over all spheres around particle A with radius r_{max}. To directly compare the MD and EXAFS structural results, the An−O and An−H $g(r)$'s are modeled with the gamma-like distributions defined as

$$f(r) = N\frac{p^{1/2}}{\sigma\Gamma(p)}\left[p + \left(\frac{r-R}{\sigma}\right)p^{1/2}\right]^{p-1}\exp\left[-p - \left(\frac{r-R}{\sigma}\right)p^{1/2}\right] \quad (4)$$

where $\Gamma(p)$ is the Euler's Gamma function for the parameter p, N is the coordination number providing the correct normalization, R is the mean distance, σ is the standard deviation, and β is the asymmetry index (third cumulant divided by σ^3) $\beta = 2p^{-1/2}$ that can be gradually varied in a wide range. Note that the R values are the average distances of the distributions that are shifted toward larger values with respect to the maximum of the $g(r)$'s due to the asymmetry. The U(III), Am(III), and Cf(III) An−O $g(r)$'s obtained from the MD simulations are shown in Figure 1 as an example, together with the asymmetric peaks obtained from the fitting procedure. The $g(r)$'s of the other actinide ions are shown in Figure S1, Supporting Information. The structural parameters obtained from the fitting of the MD $g(r)$'s are collected in Table S2, Supporting Information for the entire series.

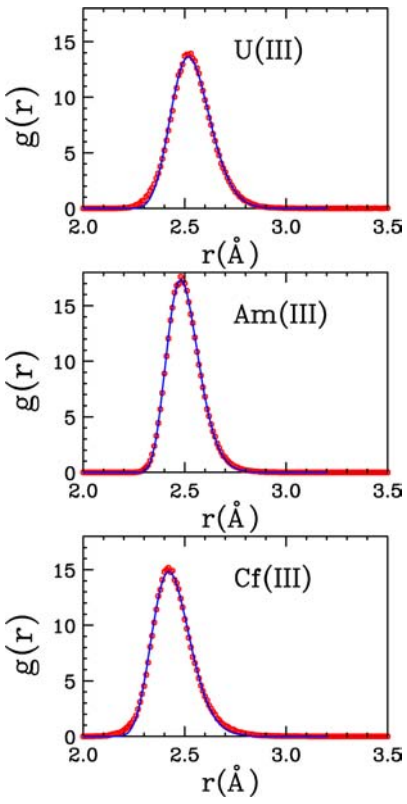

Figure 1. U(III), Am(III), and Cf(III) An−O $g(r)$'s obtained from MD simulations (red dotted line) and corresponding gamma-like asymmetric peaks obtained from the fitting procedure (blue solid line).

dx.doi.org/10.1021/ic400678u | Inorg. Chem. 2013, 52, 10318−10324

2.2. X-Absorption Measurements. The XAS absorption spectra analyzed in this work were collected by different research groups that provided us with the raw data in order to carry out a new unified EXAFS data analysis of the entire actinide series from U(III) to Cf(III). In particular, the L_3-edge XAS spectra for the U(III), Np(III), and Pu(III) ions in aqueous solution are those reported in ref 14, the XAS spectrum of Am(III) is that reported in ref 39, the XAS spectrum of Cm(III) is that reported in ref 40, the XAS spectrum of Bk(III) is that reported in ref 20, and the XAS spectrum of Cf(III) is that reported in ref 24. Experimental details on sample preparation and EXAFS data acquisition can be found in the original works.

2.3. EXAFS Data Analysis. The EXAFS data were analyzed with the latest version of the GNXAS program that can calculate phase shifts and theoretical signals also for the actinides.[41,42] The GNXAS method is based on the theoretical calculation of the EXAFS signal and subsequent refinement of the structural parameters. In this approach, interpretation of the experimental data is based on the decomposition of the $\chi(k)$ signal into a summation over n-body distribution functions, calculated by means of multiple-scattering (MS) theory. The theoretical signal $\chi(k)$ is related to the experimental absorption coefficient $\alpha(k)$ through the relation $\alpha(k) = J\sigma_0(k)[1 + S_0^2\chi(k)] + \beta(k)$, where $\sigma_0(k)$ is the atomic cross section, J is the edge jump, S_0^2 provides a uniform reduction of the signal and is associated with many-body corrections to the one-electron cross section, and $\beta(k)$ is the background function, which accounts for further absorbing processes. Multielectron excitation channels are accounted for by modeling the $\beta(k)$ function as the sum of a smooth polynomial spline and step-shaped functions. The actinide-water first coordination shells were modeled with gamma-like functions (eq 4), and both the An−O and An−H two-body contributions were included in the calculations. Phase shifts have been calculated for each system starting from one of the MD configurations, by using muffin-tin potentials and advanced models for the exchange-correlation self-energy (Hedin−Lundqvist). Inelastic losses of the photoelectron in the final state have been accounted for intrinsically by a complex potential. The model $\chi(k)$ was then refined against the experimental data using a least-squares minimization procedure in which structural and nonstructural parameters were allowed to float. Two nonstructural parameters were minimized, namely, E_0 (core ionization threshold) and S_0^2. The quality of the fits was determined by the goodness-of-the-fit parameter[41] and by careful inspection of the EXAFS residuals and their Fourier transforms (FT).

3. RESULTS AND DISCUSSION

A thorough investigation aimed at determining ionic radii in aqueous solution has been carried out by Marcus.[2] In this work the ionic radii R_{ion} were derived starting from experimental ion−water internuclear distances:

$$R_{ion} = d_{ion-water} - R_{water} \quad (5)$$

where R_{water} is a distance that characterizes the "radius" of a water molecule and $d_{ion-water}$ is an appropriate value that defines the ion−water distance and is strictly dependent on the shape of the ion−water $g(r)$'s. Application of eq 5 needs a proper choice of the R_{water} value, and different strategies have been adopted in the literature. In the original work of Marcus,[2] one uniform value of 1.39 Å was used for all ions, while in a subsequent study it was shown that the alkali metal cations and halogen anions have different R_{water} values.[43] David et al.[44] determined R_{water} by subtracting the Shannon ionic radii from the $d_{ion-water}$ distances and found that the radius of the water molecule varies between 1.34 and 1.43 Å, depending on the charge of the ion. In a recent study,[11] the ionic radii of Ln(III) ions have been determined using a R_{water} of 1.35 Å, and, due to the similarity between the two series, here we adopted the same value. A fundamental prerequisite to derive reliable ionic radii in solution is to have an accurate experimental determination of the ion−water distances. This fact has stimulated us to carry out a new careful analysis of EXAFS data for the actinide series in conjunction with MD simulations.

In recent EXAFS investigations, important information on the hydration structure of the Ln(III) series has been gained starting from crystallographic studies on the isotypic $[Ln(H_2O)_9](CF_3SO_3)_3$ (triflate) series.[45−48] In particular, it has been shown that the Ln(III) hydration complexes in aqueous solution retain a tricapped trigonal prism (TTP) geometry, in which the bonding of the capping water molecules varies along the series. Two principal structural changes occur: for the largest Ln(III) ions (La−Nd) the capping water molecules are equidistant, giving rise to a regular TTP geometry for the hydration complexes; starting at Sm(III) distortion from regular symmetry becomes evident, with one of the capping water molecules more strongly bound to the Ln(III) ion; starting at Ho(III) one of the capping water molecules is so strongly bound to the ion, as compared to the other two capping water molecules, that the occupancy of these two sites becomes lower; the last elements of the series endure a decrease of the hydration number. In analogy with the Ln(III) series, a change in the hydration numbers from nine to eight is believed to occur also for the An(III) series between Cm(III) and Es(III), although a conclusive answer has not been given.[10,13] A similar approach combining crystallographic results and structural data in aqueous solution has been used in recent investigations to shed light on the hydration properties of the An(III) ions.[23,49] Starting from the single-crystal structure of the triflate series and from 5f electronic absorption spectra, a time-averaged coordination geometry of the aqua ions similar to that of the static TTP geometry in the crystals has been suggested. Following this hypothesis, in the present work the analysis of the EXAFS data of the An(III) water solutions has been carried out assuming the existence of a TTP symmetry and using two strategies. In the former, two distinct shells accounting for the prismatic and capping oxygen atoms have been used to fit the EXAFS experimental data. In this analysis, we assumed the existence of six oxygen atoms in the prismatic sites and three oxygen atoms in the capping sites, and therefore the coordination numbers have been kept fixed during the minimization procedures. The theoretical $\chi(k)$ was calculated including both the An−O and An−H γ^2 two-body contributions and least-squares fits of the EXAFS spectra were performed in the range k = 2.0−10.3 Å^{-1}. In all cases, the quality of the spectra for k values higher than 10.3 Å^{-1} was too poor to include this energy region in the analyses. Fit procedures were applied to the whole set of structural and nonstructural parameters to improve, as far as possible, the agreement between calculated signals and experimental spectra, and a k^2 weighting was used in all the minimization procedures. The best-fit analysis of the L_3-edge EXAFS spectrum of the Cf(III) ion in aqueous solution is shown in Figure 2 as an example, while the analyses of the other actinide ions are shown in Figure S2, Supporting Information. Note that in Figure 2 the signals are shown multiplied by k^2, while in Figure S2 the data are shown multiplied by k due to the poorer quality of the spectra. The first four curves from the top of the upper panel of Figure 2 are the Cf−O(prism), Cf−O(cap), Cf−H(prism), Cf−H(cap), first-shell contributions, while the reminder of the figure shows the comparison of the total theoretical contribution with the experimental spectrum. The agreement between the experimental and the theoretical spectra is excellent; this is also evident from the corresponding Fourier

dx.doi.org/10.1021/ic400678u | Inorg. Chem. 2013, 52, 10318−10324

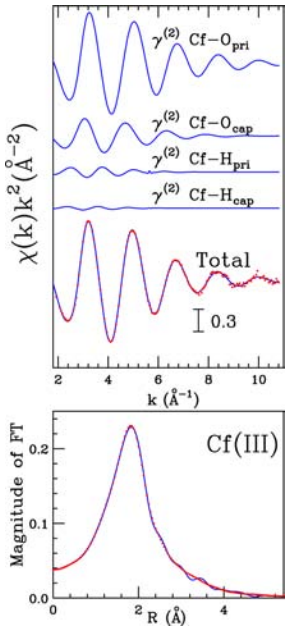

Figure 2. Upper panel: fit of the L_3-edge EXAFS spectrum of the Cf(III) ion in aqueous solution (red dotted line is experimental data, blue full line is theoretical model) using a two-shell model. Lower panel: nonphase shift corrected Fourier transform envelope function of the experimental data (red dotted line) and of the total theoretical signal (blue full line).

transform (FT) spectra shown in the lower panels of Figures 2 and S2. The FT spectra were calculated with no phase shift correction applied, in the k-range 2.0−10.0 Å^{-1}. The results of the refinements are summarized in Table 1. The standard deviations of the refined parameters do not include systematic errors of the measurements. These statistical error values allow reasonable comparisons of, for example, the significance when comparing relative shifts in the distances. However, the variations in the refined parameters, including the shift in the E_0 value (for which k = 0), with different models and data ranges, indicate that the absolute accuracy of the distances given for the separate complexes is within 0.01−0.02 Å. No uncertainties related to evaluation of data having different origins could be revealed. The fit values of S_0^2 ranged between 0.9 and 1.0 in agreement with previous determinations.[21,24] It is important to stress that the limitation of the k-range of the An(III) experimental spectra reduces the resolution and the accuracy of the analysis. Therefore, to improve the accuracy of the two-shell analysis and to resolve the prismatic and capping distances with increased sensitivity, it is necessary to collect spectra with a good signal-to-noise ratio up to k values higher than 10.0 Å^{-1}.

Table 1. Best-Fit Parameters (An−O Coordination Numbers N, Average Distances R, Debye−Waller Factors σ^2, and Asymmetry Parameter β) for the An(III) Ions in Aqueous Solution L_3-edge EXAFS Spectra, Using a Trigonal Tricapped Prism Model

	N^a	R (Å)	σ^2 (Å^2)	β
U−O_{prism}	6	2.50(1)	0.009(1)	0.2(2)
U−O_{cap}	3	2.58(2)	0.009(1)	0.1(2)
Np−O_{prism}	6	2.48(1)	0.008(1)	0.2(2)
Np−O_{cap}	3	2.56(2)	0.008(1)	0.1(2)
Pu−O_{prism}	6	2.45(1)	0.008(1)	0.1(2)
Pu−O_{cap}	3	2.55(2)	0.009(1)	0.1(2)
Am−O_{prism}	6	2.43(1)	0.008(1)	0.2(2)
Am−O_{cap}	3	2.54(2)	0.009(1)	0.1(2)
Cm−O_{prism}	6	2.40(1)	0.008(1)	0.1(2)
Cm−O_{cap}	3	2.53(2)	0.009(1)	0.1(2)
Bk−O_{prism}	6	2.38(1)	0.007(1)	0.1(2)
Bk−O_{cap}	3	2.50(2)	0.008(1)	0.1(2)
Cf−O_{prism}	6	2.37(1)	0.007(1)	0.1(1)
Cf−O_{cap}	3	2.49(2)	0.008(1)	0.1(2)

[a]The coordination numbers have been kept fixed during the minimization procedures.

The metal−oxygen distances obtained from the EXAFS data analysis for prismatically arranged and capping oxygen atoms in aqueous solutions are plotted in Figure 3 together with those of the An(III) solid triflates as determined from X-ray diffraction (XRD).[23,49]

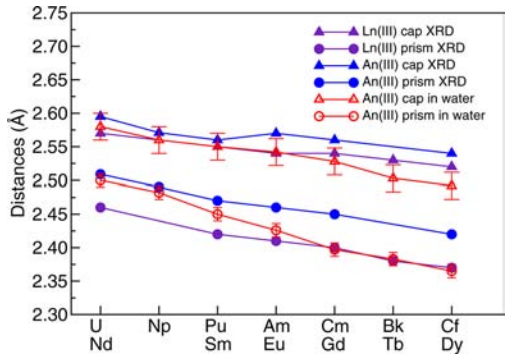

Figure 3. Prismatic and capping An−O distances in $[An(H_2O)_9](CF_3SO_3)_3$ crystals[23,49] (blue filled triangles and filled circles), prismatic and capping Ln−O distances in $[Ln(H_2O)_9](CF_3SO_3)_3$ crystals[45] (indigo filled triangles and filled circles), and prismatic and capping An−O distances for hydrated An(III) ions in solution determined from the EXAFS data analysis (red empty triangles and empty circles).

As expected, a decrease of the metal−oxygen distance takes place across the series due to the actinide contraction, similar to what is found for the Ln(III) ions. The refined structural parameters for the EXAFS models of the hydrated An(III) ions are in satisfactory agreement with those for the corresponding $[An(H_2O)_9](CF_3SO_3)_3$ crystal structures (Figure 3). However, the mean bond lengths from the EXAFS data are slightly shorter than the crystallographic results for the last members of the series starting from Pu(III). A similar trend was found also for the Ln(III) ions, and a shortening of the metal−oxygen distances was detected for hydrated ions as compared to the crystal structure starting from Sm(III), i.e., starting at the element with f^6 electronic structure as does Pu(III).[45] This deviation suggests that one capping water molecule is more strongly bound to the An(III) ion, thus determining a shortening of the measured An−O distance compared to the crystal structure.

In Figure 3 we also report the Ln−O crystallographic distances obtained for the $[Ln(H_2O)_9](CF_3SO_3)_3$ crystals. The Ln-O distances determined for the solid triflates are systematically shorter than the An-O ones. In particular, a decrease of 0.05 Å and 0.02/0.03 Å is detected for the prismatic and capping positions, respectively. A different result has been obtained in aqueous solution as can be observed looking at

dx.doi.org/10.1021/ic400678u | Inorg. Chem. 2013, 52, 10318−10324

Figure 4 where the prismatic and capping metal−oxygen distances obtained for the An(III) ions in water are compared

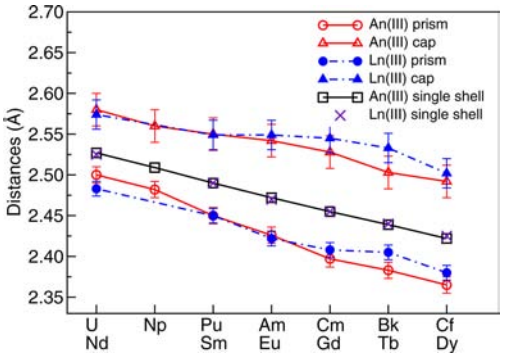

Figure 4. Prismatic and capping ion−O distances for the An(III) and Ln(III) ions[13] in water determined from the EXAFS data analysis. The An−O and Ln−O distances[13] obtained from the single shell analysis are also reported.

with those previously determined for the Ln(III) ions.[10] In both cases the capping distances are approximately 0.1 Å longer than the prismatic ones and the distances obtained for the actinides follow closely their lanthanide counterparts. This result is a first indication that the two series show similar hydration properties. We note that the distortion from the TTP symmetry and the decrease of coordination number that take place in the lanthanide series after Ho(III) are not observed for the investigated actinide ions. This means that the corresponding coordination transition in the actinide series, if present, arises after Cf(III).

In the second strategy, a single-shell model was used in the EXAFS analysis of the An(III) aqueous solutions, with the aim of extracting an accurate An−O distance to be used in the calculation of the ionic radii. Given the C_{3h} symmetry of the An(III) hydration complexes, the distribution of oxygen atoms around the ions is expected to be asymmetric. In a previous EXAFS work dealing with Ln(III) ions in water, it was shown that the effect of asymmetry becomes evident in the k range above 10 Å^{-1} (see Figure 7 of ref 46). As mentioned above, the quality of the An(III) spectra allowed us to analyze the EXAFS data only up to 10.3 Å^{-1}. As a consequence, it is not possible to obtain an accurate determination of the asymmetry parameter β from the experimental data, and we resorted to using the results obtained from the MD simulation as constraints in the EXAFS refinements. In particular, we fixed the β values to those obtained from the MD simulations (see Table S2, Supporting Information), to properly account for the asymmetry of the hydration shells, that cannot be retrieved from the EXAFS data due to the limitation of the analyzable k range. This constrained minimization of the EXAFS spectra increases the accuracy of the analysis allowing a more accurate determination of the An−O distance. Moreover, this combined analysis allows one to properly account both for the dynamic behavior of the system probed by the MD simulation and for a possible decrease of the hydration number across the actinide series.

The results of the single-shell analysis are shown in Figure 5, where the total theoretical EXAFS signals are compared to the experimental data. Note that the theoretical model contains both the ion-oxygen and the ion-hydrogen signals. The agreement between experimental and theoretical spectra is excellent. The An−O structural parameters obtained from this

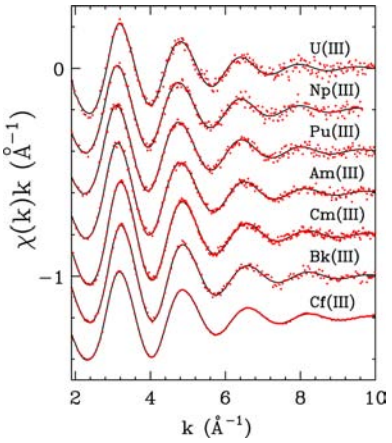

Figure 5. L_3-edge experimental EXAFS spectra of An(III) ions in aqueous solutions (black points) and fitted curves (solid line) obtained from the single shell analysis.

analysis for the series are reported in Table 2 together with the values reported in the literature. Note that the An−O distances

Table 2. Best-Fit An−O First Shell Structural Parameters of An(III) Ions in Aqueous Solution Determined from the EXAFS Analysis Using a Single Shell Model[a]

	R (Å)	σ^2 (Å^2)	β[b]	R_l (Å)	IR (Å)
U(III)	2.527(9)	0.010(2)	0.40	2.52[c]	1.177
				2.56[d]	
Np(III)	2.509(9)	0.010(2)	0.42	2.48[e]	1.159
				2.52[c,d]	
Pu(III)	2.490(9)	0.010(2)	0.44	2.49[c,f]	1.140
				2.51[d,g,h]	
Am(III)	2.472(8)	0.009(2)	0.49	2.48[h,i]	1.122
Cm(III)	2.455(8)	0.009(2)	0.47	2.45[h]	1.105
				2.47[j]	
Bk(III)	2.439(8)	0.009(2)	0.46	2.43[k]	1.089
Cf(III)	2.422(7)	0.008(2)	0.45	2.42[l,m]	1.072

[a]Coordination numbers were kept fixed to 9, R is the average distance, σ^2 is the Debye−Waller factor, and β is the asymmetry parameter. An−O distances obtained from literature sources are also reported (R_l), together with the ionic radii (IR) of actinide(III) ions in aqueous solution as determined in the present work. [b]The β parameters were fixed to the values determined from MD simulations (see Table S2, Supporting Information). [c]Reference 14. [d]Reference 16. [e]Reference 19. [f]Reference 17. [g]Reference 15. [h]Reference 18. [i]Reference 39. [j]Reference 21. [k]Reference 20. [l]Reference 23. [m]Reference 24.

obtained from the present analysis are in agreement with the average values previously determined for all the investigated ions. Also in this case, the fit values of S_0^2 ranged between 0.9 and 1.0. In Figure 4, the An−O distances obtained from the single-shell analysis are compared to Ln−O distances.[11] The first shell distances of the An(III) hydration complexes are practically identical to the Ln(III) counterparts, reflecting the similar hydration properties of the two series. As previously found for the Ln(III) ions, the uncertainty in the coordination numbers obtained from EXAFS is too large for a conclusive determination of the hydration complex geometry.[45,46] As a consequence, the mean metal−oxygen bond length obtained from the EXAFS analysis is a more reliable indicator of the coordination number than the direct determination of the number of coordinating ligands. Comparison of the EXAFS

dx.doi.org/10.1021/ic400678u | Inorg. Chem. 2013, 52, 10318−10324

distances obtained for An(III) aqua ions with those for the Ln(III) ions clearly indicates the existence of a 9-fold TTP coordination for all the actinide ions in solution up to Cf(III), in agreement with previous hypotheses based on single-crystal X-ray structures of An(III) triflates.

Starting from these results, we calculated a new set of ionic radii for the An(III) ions in aqueous solution using eq 5 (see Table 2 and Figure 6). As previously mentioned, we adopted a

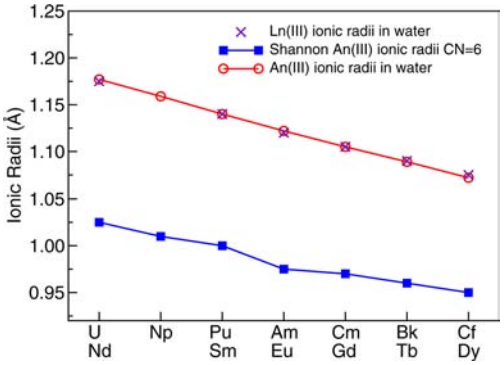

Figure 6. Ionic radii of An(III) ions in aqueous solution compared to Ln(III) ionic radii in aqueous solution, and the Shannon 6-fold crystal ionic radii.[1]

R_{water} value of 1.350 Å that corresponds to the Shannon radius of a coordinated oxygen atom. In Figure 6, the An(III) and Ln(III) ionic radii in water are compared and shown together with the crystal ionic radii determined by Shannon for crystalline compounds in which the An(III) ions are six-coordinated. Note that for the actinide series no 8-fold or 9-fold crystal ionic radii are available in the literature due to the lack of a sufficient number of single crystal structures of actinide inorganic compounds. As expected, the An(III) ionic radii in aqueous solution show a regular trend; they decrease smoothly with increasing atomic number. Moreover, the major result of this investigation is the evidence for a close similarity between the ionic radii in aqueous solution of An(III) and Ln(III) ions through the series, reflecting the electrostatic nature of the Ln/An−O bonds. While performing electronic structure calculations on cations in a vacuum, the authors found that An(III) ions are more polarizable than Ln(III),[10,50] apparently this property has a minor impact on hydration properties. As reported by different authors from both theoretical[38,51,52] and experimental[49,53] studies, this is probably due to the strong electrostatic character of the ion−water interaction. In particular, while the ion polarization itself plays a minor role, the 3+ charge on the ion strongly polarizes the surrounding water molecules, as reported from classical[38,54,33] and DFT-based[52] simulations. Triply charged ions strongly modify (of about 0.5 D) the dipoles of water molecules in the first hydration shell with respect to bulk water, while the dipole on the ion is small. This reflects the hard character of Ln(III)/An(III)-water interaction due to the fact that 4f and 5f orbitals are compact and their effect on hydration is negligible. Thus, when the lanthanide and actinide ions have the same 3+ charge, they behave similarly in water and this is reflected in the ionic radius values.

A last remark we would like to make concerns the different behavior that can be observed when looking at the structures of the An(III) and Ln(III) triflate salts. The An−O distances determined for the triflate crystals are systematically longer than the Ln−O ones (see Figure 3). This finding demonstrates that the "crystal ionic radii" of ions determined from crystallographic structures are not always valid as descriptors of ions in electrolyte solutions. In the most valid review dealing with ionic radii in aqueous solution, Marcus states: "Referring back to the usually employed crystal ionic radii, only if their validity for expressing the radii of the ions in solution is demonstrated for a wide variety of ions on the basis of experimental evidence can the implicit assumption of the validity of the use of crystal ionic radii in lieu of the solution ionic radii be maintained."[2] From the results of the present work, it appears that for the actinide series the ionic radii determined in crystalline compounds are not transferable to triply charged ions in aqueous solution.

4. CONCLUDING REMARKS

In conclusion, we have determined the structural hydration properties of the actinide ions from U(III) to Cf(III) in a unique and coherent way. EXAFS data have been used in combination with state of the art MD simulations to increase the accuracy of the measured An−O distances compared to previous experimental determinations. This systematic study reveals a strong analogy between the Ln(III) and An(III) series concerning hydration properties. The existence of a contraction of the An−O distance along the series has been highlighted, while no decrease of the hydration number is evident up to Cf(III). Finally, in this work, we present the first experimental determination of the ionic radii of the An(III) ions in water from U(III) to Cf(III). Assuming the same radius of coordinating water molecules, the An(III) and Ln(III) series have been found to have almost identical ionic radii. This allows us to conclude that the two series behave very similarly in water with respect to hydration structural and thermodynamical properties. This justifies from the experimental point of view the use of Ln(III) ions as analogues of An(III) ions, which can be useful since the former elements are easier to find and manipulate than the latter. This analogy, on the other hand, represents a challenge for separation techniques, whose efficiency rests on dissimilar behavior in different solvents and/or specific molecules able to differentiate between such very similar hard cations.

■ ASSOCIATED CONTENT

Ⓢ Supporting Information

Tables S1 and S2 and Figures S1 and S2. This material is available free of charge via the Internet at http://pubs.acs.org.

■ AUTHOR INFORMATION

Corresponding Author

*E-mail: p.dangelo@caspur.it. Fax:+39-06-49913751.

Notes

The authors declare no competing financial interest.

■ ACKNOWLEDGMENTS

The authors are indebted to Dr. Lynda Soderholm and Dr. Mark Antonio for providing the Bk experimental spectrum and to Prof. Christophe Den Auwer for providing the Cf experimental spectrum. The Cf spectrum, as well as the EXAFS of the remaining actinides in this study, are available from 'AcXAS', an Actinide Reference X-ray Absorption Spectroscopy Database, https://www.hzdr.de/acxas. This work was partially supported (F.M. and R.S.) by the ANR

2010 JCJC 080701 ACLASOLV (Actinoids and Lanthanoids Solvation) and by the University of Rome "La Sapienza" (Progetto ateneo 2012, n. C26A129ZAY) (P.D.).

REFERENCES

(1) Shannon, R. D. *Acta Crystallogr. A* **1976**, *32*, 751−767.
(2) Marcus, Y. *Chem. Rev.* **1988**, *88*, 1475−1498.
(3) Heyrovska, R. *Chem. Phys. Lett.* **2006**, *429*, 600−605.
(4) Migliorati, V.; Mancini, G.; Chillemi, G.; Zitolo, A.; D'Angelo, P. *J. Phys. Chem. A* **2011**, *115*, 4798−4803.
(5) D'Angelo, P.; Migliorati, V.; Guidoni, L. *Inorg. Chem.* **2010**, *49*, 4224−4231.
(6) D'Angelo, P.; Migliorati, V.; Mancini, G.; Barone, V.; Chillemi, G. *J. Chem. Phys.* **2008**, *128*, 084502.
(7) Spezia, R.; Duvail, M.; Vitorge, P.; Cartailler, T.; Tortajada, J.; Chillemi, G.; D'Angelo, P.; Gaigeot, M. P. *J. Phys. Chem. A* **2006**, *110*, 13081−13088.
(8) Migliorati, V.; Mancini, G.; Tatoli, S.; Zitolo, A.; Filipponi, A.; De Panfilis, S.; Di Cicco, A.; D'Angelo, P. *Inorg. Chem.* **2013**, *52*, 1141−1150.
(9) D'Angelo, P.; Migliorati, V.; Mancini, G.; Chillemi, G. *J. Phys. Chem. A* **2008**, *112*, 11833−11841.
(10) Duvail, M.; Martelli, F.; Vitorge, P.; Spezia, R. *J. Chem. Phys.* **2011**, *135*, 044503.
(11) D'Angelo, P.; Zitolo, A.; Migliorati, V.; Chillemi, G.; Duvail, M.; Vitorge, P.; Abadie, S.; Spezia, R. *Inorg. Chem.* **2011**, *50*, 4572−4579.
(12) Lundberg, D.; Persson, I.; Eriksson, L.; D'Angelo, P.; De Panfilis, S. *Inorg. Chem.* **2010**, *49*, 4420−4432.
(13) D'Angelo, P.; Spezia, R. *Chem.—Eur. J.* **2012**, *18*, 11162−11178.
(14) Brendebach, B.; Banik, N. L.; Marquardt, C. M.; Rothe, J.; Denecke, M.; Geckeis, H. *Radiochim. Acta* **2009**, *97*, 701−708.
(15) Allen, P. G.; Bucher, J. J.; Shuh, D. K.; Edelstein, N. M.; Reich, T. *Inorg. Chem.* **1997**, *36*, 4676−4683.
(16) David, F.; Revel, R.; Fourest, B.; Hubert, S.; Le Du, J. F.; Den Auwer, C.; Madic, C.; Morss, L. R.: Ionova, G.; Mikhalko, V.; Vokhmin, V.; Nikonov, M.; Berthet, J. C.; Ephritikhine, M. In *Speciation, Techniques and Facilities for Radioactive Materials at Synchrotron Light Sources*; Nuclear Energy Agency: Organisation for Economic Co-Operation and Development: Grenoble, France, 1998; pp 95−100.
(17) Conradson, S. D. *Appl. Spectrosc.* **1998**, *52*, 252A−279A.
(18) Allen, P.; Bucher, J. J.; Shuh, D. K.; Edelstein, N. M.; Craig, I. *Inorg. Chem.* **2000**, *39*, 595−601.
(19) Antonio, M.; Soderholm, L.; Williams, C. W.; Blaudeau, J.-P.; Bursten, B. *Radiochim. Acta* **2001**, *89*, 17−25.
(20) Antonio, M.; Williams, C. W.; Soderholm, L. *Radiochim. Acta* **2002**, *90*, 851−856.
(21) Skanthakumar, S.; Antonio, M.; Wilson, R.; Soderholm, L. *Inorg. Chem.* **2007**, *46*, 3485−3491.
(22) Revel, R.; Den Auwer, C.; Madic, C.; David, F.; Fourest, B.; Hubert, S.; Du, J.; Morss, L. R. *First Inorg. Chem.* **1999**, *38*, 4139−4141.
(23) Lindqvist-Reis, P.; Apostolidis, C.; Rebizant, J.; Morgenstern, A.; Klenze, R.; Walter, O.; Fanghnel, T.; Haire, R. G. *Angew. Chem., Int. Ed.* **2007**, *46*, 919−922.
(24) Galbis, E.; Hernandez-Cobos, J.; Den Auwer, C.; Naour, C. L.; Guillaumont, D.; Simoni, E.; Pappalardo, R. R.; Sanchez-Marcos, E. *Angew. Chem., Int. Ed.* **2010**, *49*, 3811−3815.
(25) Hagberg, D.; Bednarz, F.; Edelstein, N. M.; Gagliardi, L. *J. Am. Chem. Soc.* **2007**, *129*, 14136−14137.
(26) Atta-Fynn, R.; Bylaska, E. J.; Shenter, W. G.; de Jong, K. A. *J. Phys. Chem. A* **2011**, *115*, 4665−4677.
(27) Wiebke, J.; Moritz, A.; Cao, X.; Dolg, M. *Phys. Chem. Chem. Phys.* **2007**, *9*, 459−465.
(28) Thole, B. T. *Chem. Phys.* **1981**, *59*, 341−350.
(29) Jorgensen, W. L.; Chandrasekhar, J.; Madura, J. D.; Impey, R. W.; Klein, M. L. *J. Chem. Phys.* **1983**, *79*, 926−935.
(30) van Duijnen, P.; Swart, M. *J. Phys. Chem. A* **1998**, *102*, 2399−2407.
(31) Duvail, M.; Souaille, M.; Spezia, R.; Cartailler, T.; Vitorge, P. *J. Chem. Phys.* **2007**, *127*, 034503.
(32) Martelli, F.; Vuilleumier, R.; Simonin, J.-P.; Spezia, R. *J. Chem. Phys.* **2012**, *137*, 164501.
(33) Martelli, F.; Abadie, S.; Simonin, J.-P.; Vuilleumier, R.; Spezia, R. *Pure Appl. Chem.* **2013**, *85*, 237−246.
(34) Essmann, U.; Perera, L.; Berkowitz, M. L.; Darden, T.; Lee, H.; Pedersen, L. G. *J. Chem. Phys.* **1995**, *103*, 8577.
(35) Sprik, M. *J. Phys. Chem.* **1991**, *95*, 2283−2291.
(36) Souaille, M.; Loirat, H.; Borgis, D.; Gaigeot, M.-P. *Comput. Phys. Commun.* **2009**, *180*, 276−301.
(37) Duvail, M.; Spezia, R.; Vitorge, P. *ChemPhysChem* **2008**, *9*, 693−696.
(38) Duvail, M.; Vitorge, P.; Spezia, R. *J. Chem. Phys.* **2009**, *130*, 104501.
(39) Stumpf, S.; Stumpf, T.; Dardenne, K.; Hennig, C.; Foerstendorf, H.; Klenze, R.; Fanghanel, T. *Environ. Sci. Technol.* **2006**, *40*, 3522−3528.
(40) Weigl, M.; Denecke, M. A.; Panak, P. J.; Geist, A.; Gompper, K. *Dalton Trans.* **2005**, 1281−1286.
(41) Filipponi, A.; Cicco, A. D. *Phys. Rev. B* **1995**, *52*, 15135−15149.
(42) Filipponi, A.; Cicco, A. D.; Natoli, C. R. *Phys. Rev. B* **1995**, *52*, 15122−15134.
(43) Heyrovska, R. *Chem. Phys. Lett.* **1989**, *163*, 207−211.
(44) David, F.; Vokhmin, V.; Ionova, G. *J. Mol. Liq.* **2001**, *90*, 45−62.
(45) Persson, I.; D'Angelo, P.; De Panfilis, S.; Sandstrom, M.; Eriksson, L. *Chem.—Eur. J.* **2008**, *14*, 3056−3066.
(46) D'Angelo, P.; De Panfilis, S.; Filipponi, A.; Persson, I. *Chem.—Eur. J.* **2008**, *14*, 3045−3055.
(47) D'Angelo, P.; Zitolo, A.; Migliorati, V.; Mancini, G.; Persson, I.; Chillemi, G. *Inorg. Chem.* **2009**, *48*, 10239−10248.
(48) D'Angelo, P.; Zitolo, A.; Migliorati, V.; Persson, I. *Chem.—Eur. J.* **2010**, *16*, 684−692.
(49) Apostolidis, C.; Schimmelpfennig, B.; Magnani, N.; Lindqvist-Reis, P.; Walter, O.; Sykora, R.; Morgenstern, A.; Colineau, E.; Caciuffo, R.; Klenze, R.; Haire, R. G.; Rebizant, J.; Bruchertseifer, F.; Fanghnel, T. *Angew. Chem., Int. Ed.* **2010**, *49*, 6343−6347.
(50) Clavagura, C.; Dognon, J.-P. *Chem. Phys.* **2005**, *311*, 169−176.
(51) Kuta, J.; Clark, A. E. *Inorg. Chem.* **2010**, *49*, 7808−7817.
(52) Terrier, C.; Vitorge, P.; Gaigeot, M.-P.; Spezia, R.; Vuilleumier, R. *J. Chem. Phys.* **2010**, *133*, 044509.
(53) Dupouy, G.; Bonhoure, I.; Conradson, S. D.; Dumas, T.; Hennig, C.; Le Naour, C.; Moisy, P.; Petit, S.; Scheinost, A.; Simoni, E.; Den Auwer. *Eur. J. Inorg. Chem.* **2011**, 1560−1569.
(54) Villa, A.; Hess, B.; Saint-Martin, H. *J. Phys. Chem. B* **2009**, *113*, 7270−7281.